Electronic Supplementary Material (ESI) for Journal of Materials Chemistry C.

Supporting Information for

Covalent chemical functionalization of $Ti_3C_2T_x$ MXene nanosheets with fullerenes C_{60} and C_{70} for enhanced nonlinear optical limiting

Yan Fang,[†] *Zhiyuan Wei,*[†] *Zihao Guan,*[†] *Naying Shan,*[†] *Yang Zhao,*[†] *Fang Liu,*[†] *Lulu Fu,*[†] *Zhipeng Huang,*[†] *Mark G. Humphrey,*[‡] *Chi Zhang*,*[†]

[†] China-Australia Joint Research Center for Functional Molecular Materials, School of Chemical Science and Engineering, Tongji University, Shanghai 200092, China

[‡] Research School of Chemistry, Australian National University, Canberra, ACT 2601, Australia

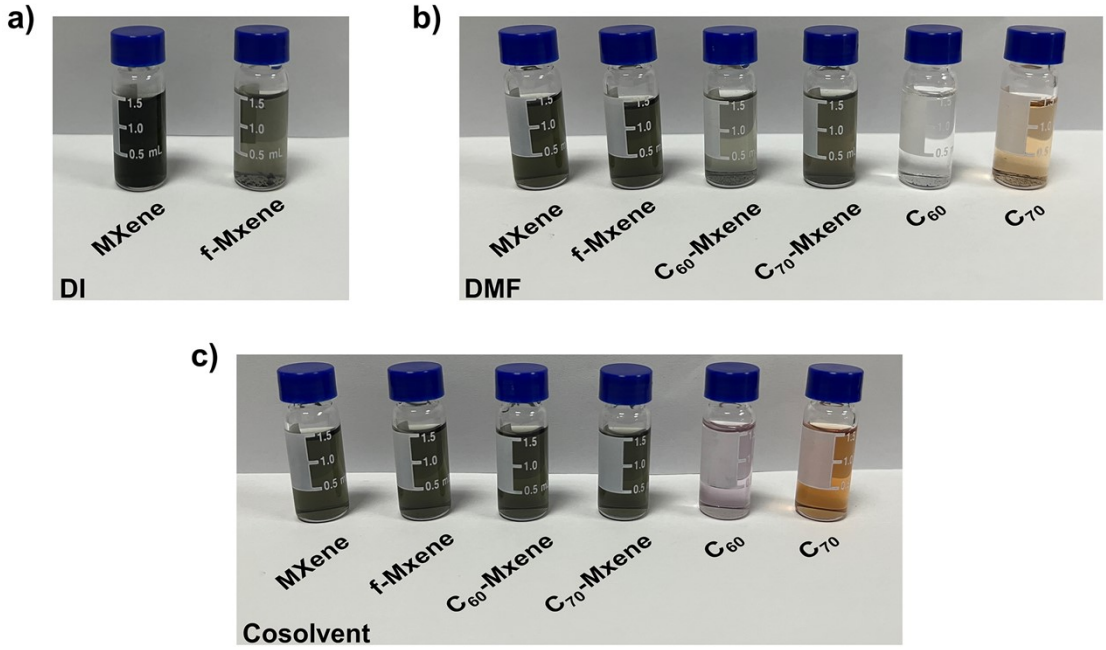

Figure S1. a) Photographs of MXene and f-MXene dispersions, with deionized water (DI) as the solvent. b) Photographs of MXene, f-MXene, C_{60}-MXene, and C_{70}-MXene dispersions, as well as C_{60} and C_{70} solutions, with N, N-dimethylformamide (DMF) as the solvent. c) Photographs of MXene, f-MXene, C_{60}-MXene, and C_{70}-MXene dispersions, as well as C_{60} and C_{70} solutions, with the cosolvent (DMF/Toluene = 2 : 1, volume ratio) as the solvent. MXene-based samples are all at the same concentration of 0.1 mg ml^{-1}. C_{60} and C_{70} solutions are with a concentration of 0.5 mg ml^{-1}.

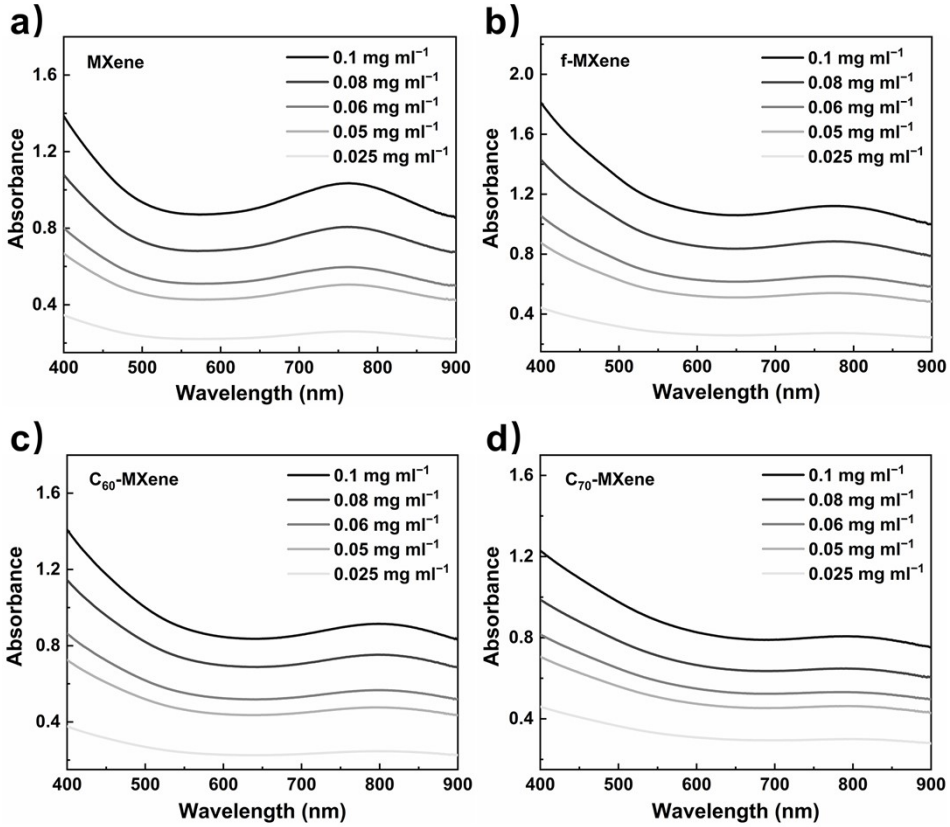

Figure S2. Concentration dependence of absorption spectra of a) MXene, b) f-MXene, c) C_{60}-MXene, and d) C_{70}-MXene in the cosolvent.

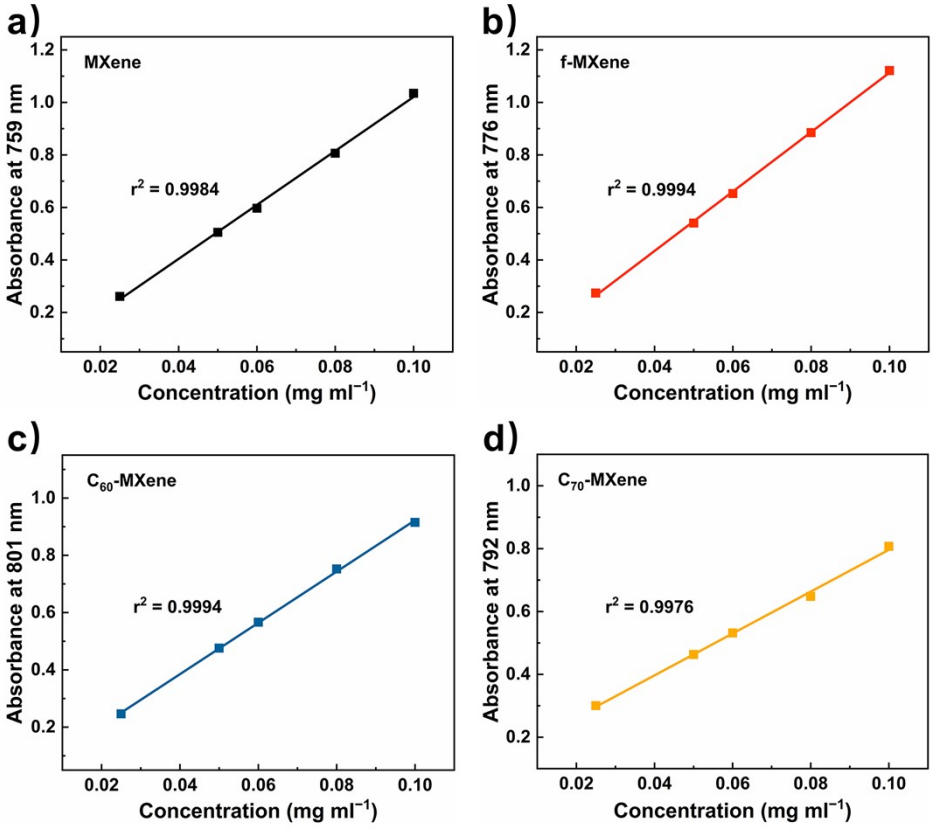

Figure S3. The absorbance of a) MXene, b) f-MXene, c) C_{60}-MXene, and d) C_{70}-MXene at different concentrations at their respective peak position around 800 nm. The straight lines are the linear fitting results of the data.

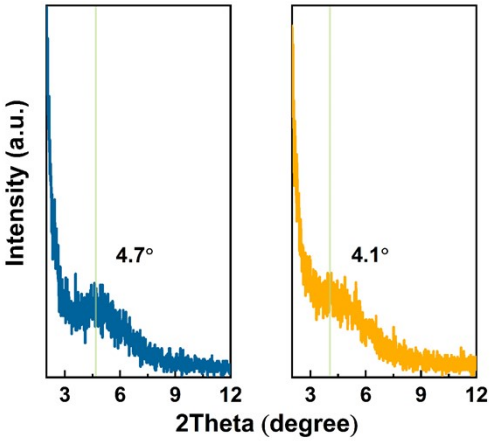

Figure S4. Low-angle XRD results for a) C_{60}-MXene and b) C_{70}-MXene.

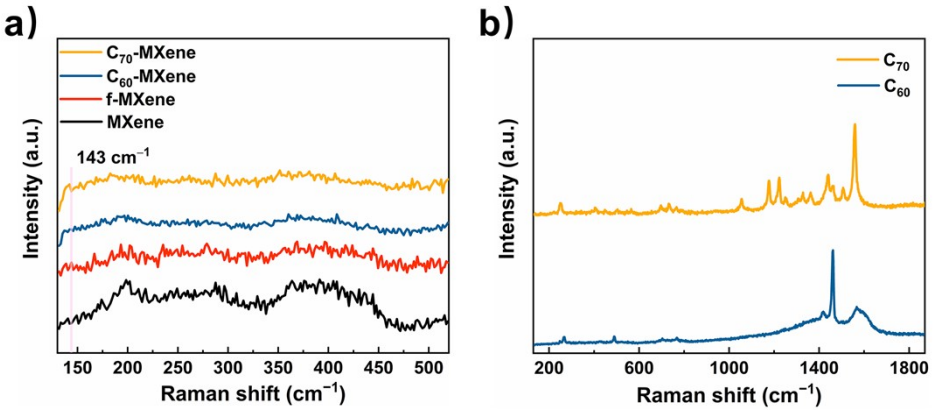

Figure S5. a) Raman spectra of MXene, f-MXene, C_{60}-MXene, and C_{70}-MXene in the low-wavenumber region, and an absence of signal at 143 cm^{-1} in all samples indicates a negligible existence of TiO_2. b) Raman spectra of fullerenes C_{60} and C_{70}.

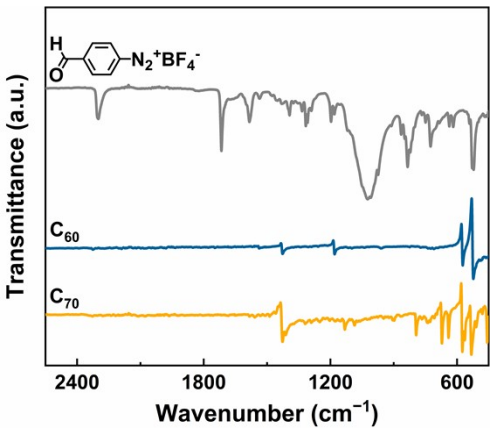

Figure S6. ATR-IR spectra of 4-benzaldehyde diazonium tetrafluoroborate, C_{60}, and C_{70}.

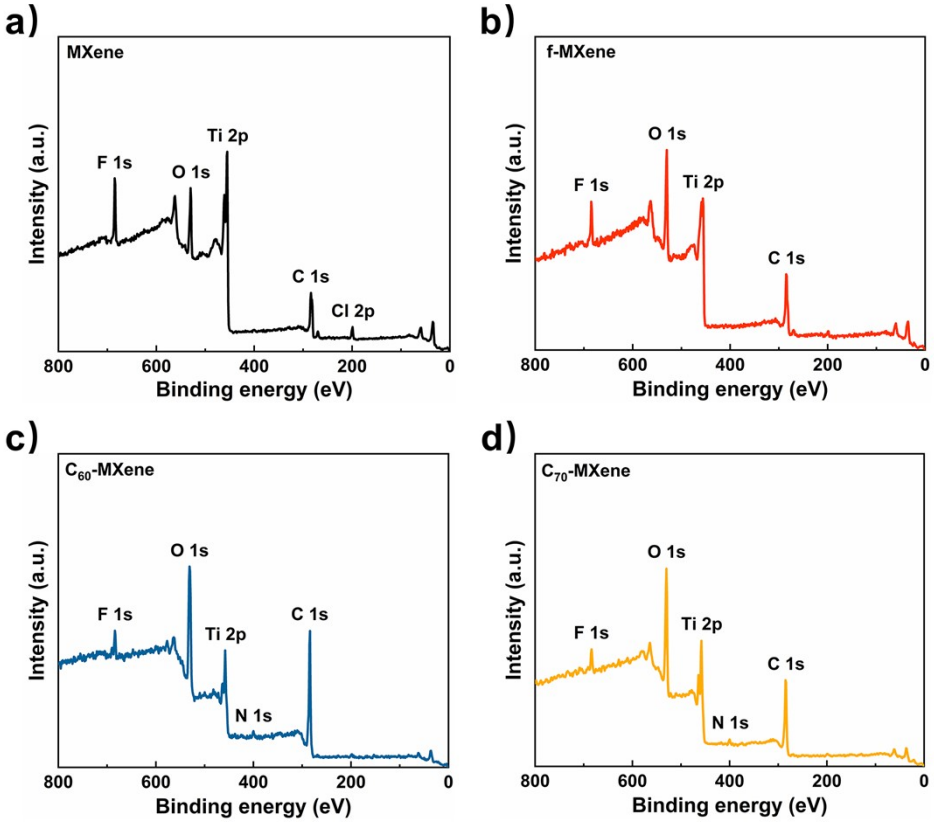

Figure S7. XPS survey spectra of a) MXene, b) f-MXene, c) C_{60}-MXene, and d) C_{70}-MXene.

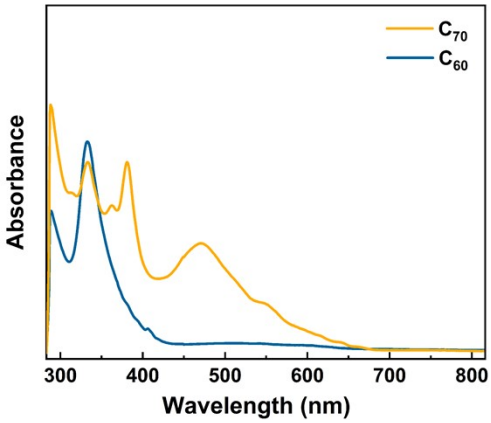

Figure S8. The absorption spectra of fullerenes C_{60} and C_{70}.

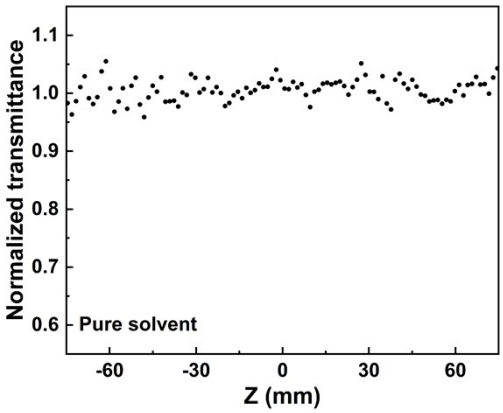

Figure S9. Z-scan data of pure solvent under the ns laser with an input intensity of 105 μJ.

Section S1. Data fitting of Z-scan curves.

The total absorption coefficient of a given material can be written as

$$\alpha(I) = \alpha_0 + \beta I, \qquad \text{(Equation S1)}$$

where α_0 and β correspond to linear absorption coefficient and nonlinear absorption coefficient, respectively. I is the incident light intensity. The light propagation model in the measured sample can be expressed as[1]

$$\frac{dI}{dz} = -(\alpha_0 + \beta I)I, \qquad \text{(Equation S2)}$$

For the open-aperture Z-scan technique, the normalized transmittance is given as[1]

$$T(z) = \sum_{m=0}^{\infty} \frac{[\frac{-\beta I_0 L_{eff}}{1 + z^2/z_0^2}]^m}{(m+1)^{3/2}}, \qquad \text{(Equation S3)}$$

where $L_{eff} = (1 - e^{-\alpha_0 L})/\alpha_0$ is the effective interaction length, α_0 stands for the linear absorption coefficient, L is the sample thickness, β is the nonlinear absorption coefficient, I_0 is the on-axis peak laser intensity at the focal point, and z_0 is the Rayleigh diffraction length.

By fitting the experimental Z-scan potints, β can be obtained. The imaginary part of the third-order nonlinear susceptibility ($Im\chi^{(3)}$) is calculated according to[2]

$$Im\chi^{(3)} = \left[\frac{10^{-7} C\lambda n^2}{96\pi^2}\right]\beta, \qquad \text{(Equation S4)}$$

where c is the speed of light, λ is the excitation wavelength, and n is the refractive index.

For obtaining the nonlinear refractive index (n_2), the closed-aperture Z-scan data is fitted with the formula[1]

$$T_{close/open} = 1 + \frac{4(z/z_0)\Delta\phi}{(z^2/z_0^2 + 9)(z^2/z_0^2 + 1)}, \qquad \text{(Equation S5)}$$

where $T_{close/open}$ is the normalized transmittance for the sample at the z point and $\Delta\phi = 2\pi n_2 I_0 L_{eff}/\lambda$ stands for the nonlinear phase shift.

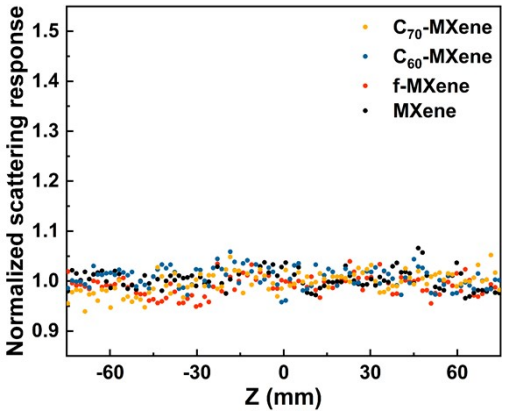

Figure S10. Z-scan scattering results of MXene, f-MXene, C_{60}-MXene, and C_{70}-MXene dispersions under ns pulses with a fluence energy of 105 μJ.

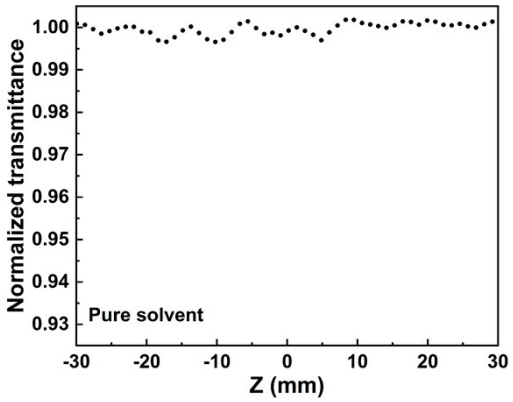

Figure S11. Z-scan data of pure solvent under the fs laser with an input intensity of 136 nJ.

Table S1. Nonlinear optical parameters of measured samples based on the fitting of open-aperture Z-scan data.

Samples	Laser	E_{pulse} (μJ)	T_0	β (cm GW^{-1})	Im$\chi^{(3)}$ (× 10^{-11} esu)
MXene	532 nm 12 ns 10 Hz	105	0.72	34.9 ± 1.9	1.23 ± 0.07
f-MXene			0.73	31.0 ± 1.7	1.09 ± 0.06
C_{60}			0.76	26.2 ± 1.2	0.92 ± 0.04
C_{70}			0.69	41.7 ± 1.5	1.46 ± 0.05
C_{60}/MXene			0.72	35.8 ± 2.5	1.26 ± 0.09
C_{70}/MXene			0.69	45.7 ± 2.5	1.61 ± 0.09
C_{60}-MXene			0.59	74.9 ± 1.8	2.63 ± 0.06
C_{70}-MXene			0.60	70.0 ± 1.8	2.46 ± 0.06
MXene	800 nm 34 fs 1 kHz	136 × 10^{-3}	0.95	(1.70 ± 0.07) × 10^{-3}	(0.97 ± 0.04) × 10^{-4}
f-MXene			0.95	(1.81 ± 0.06) × 10^{-3}	(1.03 ± 0.03) × 10^{-4}
C_{60}			—	—	—
C_{70}			—	—	—
C_{60}/MXene			0.95	(1.54 ± 0.06) × 10^{-3}	(0.88 ± 0.03) × 10^{-4}
C_{70}/MXene			0.95	(1.82 ± 0.05) × 10^{-3}	(1.03 ± 0.03) × 10^{-4}
C_{60}-MXene			0.93	(3.26 ± 0.09) × 10^{-3}	(1.85 ± 0.05) × 10^{-4}
C_{70}-MXene			0.93	(2.80 ± 0.12) × 10^{-3}	(1.59 ± 0.07) × 10^{-4}

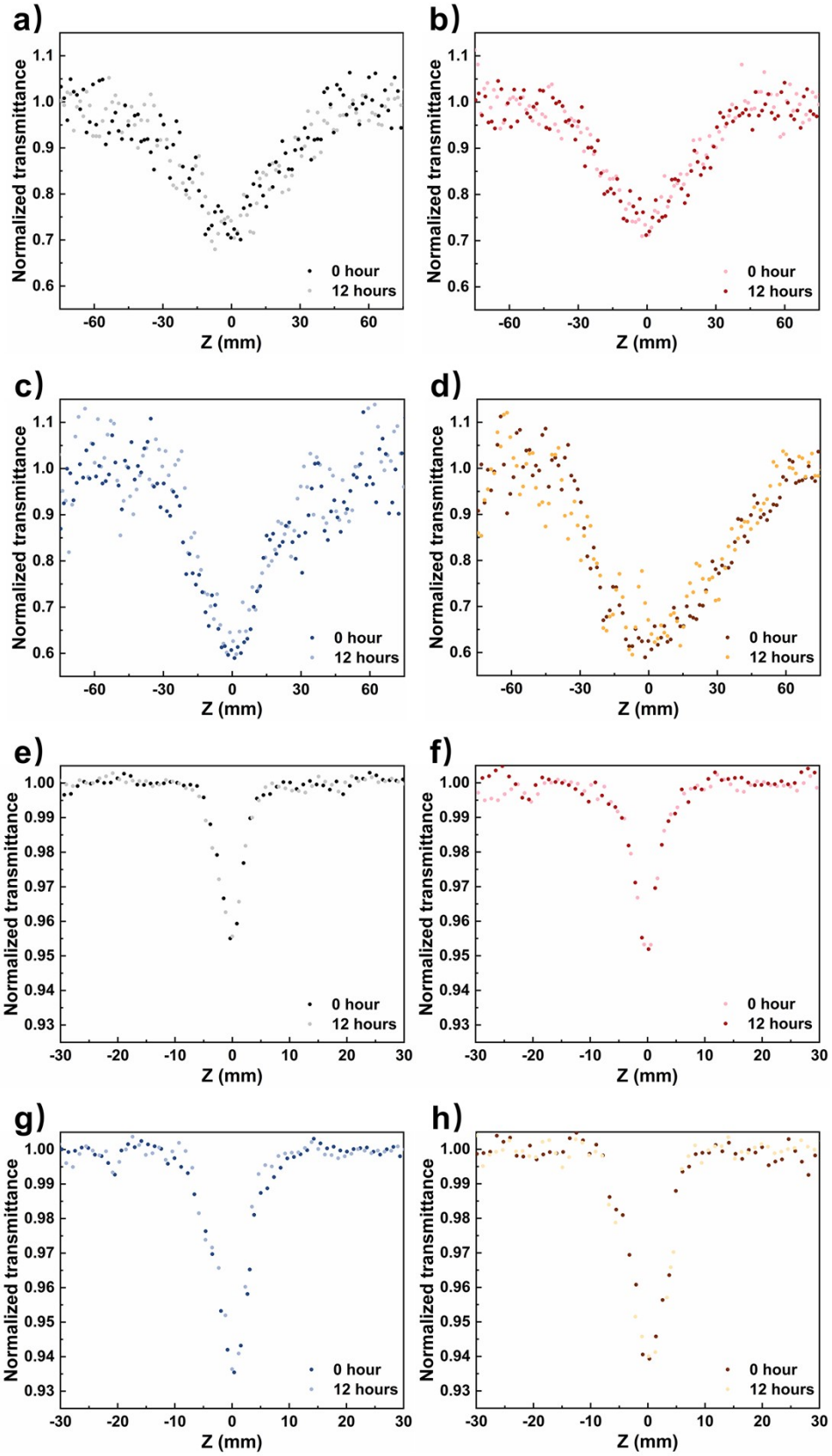

Figure S12. Z-scan results of a) MXene, b) f-MXene, c) C_{60}-MXene, and d) C_{70}-MXene under the ns laser with an input energy of 105 μJ. e), f), g), and h) are Z-scan results of MXene, f-MXene, C_{60}-MXene, and C_{70}-MXene, respectively, under the fs laser with an input energy of 136 nJ.

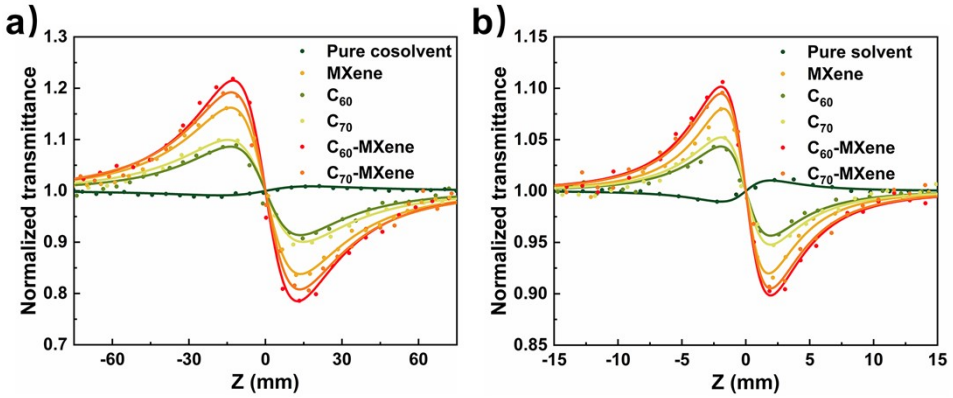

Figure S13. The results of closed-aperture Z-scan measurements under a) ns pulses at 532 nm with the input energy of 105 μJ and b) fs pulses at 800 nm with the input energy of 136 nJ. Solid lines are fitted curves.

Table S2. The nonlinear refractive indexes (n_2) of measured samples based on the fitting of closed-aperture Z-scan data.

Samples	**Laser**	E_{pulse} **(μJ)**	n_2 **(** $\times$ 10^{-3} **cm² GW⁻¹)**
MXene	532 nm 12 ns 10 Hz	105	−2.23 ± 0.16
C_{60}			−1.19 ± 0.07
C_{70}			−1.47 ± 0.09
C_{60}-MXene			−2.73 ± 0.09
C_{70}-MXene			−2.59 ± 0.08
Pure solvent			0.16 ± 0.01
MXene	800 nm 34 fs 1 kHz	136 × 10^{-3}	(−7.60 ± 0.23) × 10^{-4}
C_{60}			(−3.34 ± 0.21) × 10^{-4}
C_{70}			(−4.02 ± 0.39) × 10^{-4}
C_{60}-MXene			(−9.82 ± 0.53) × 10^{-4}
C_{70}-MXene			(−7.91 ± 0.55) × 10^{-4}
Pure solvent			(0.79 ± 0.06) × 10^{-4}

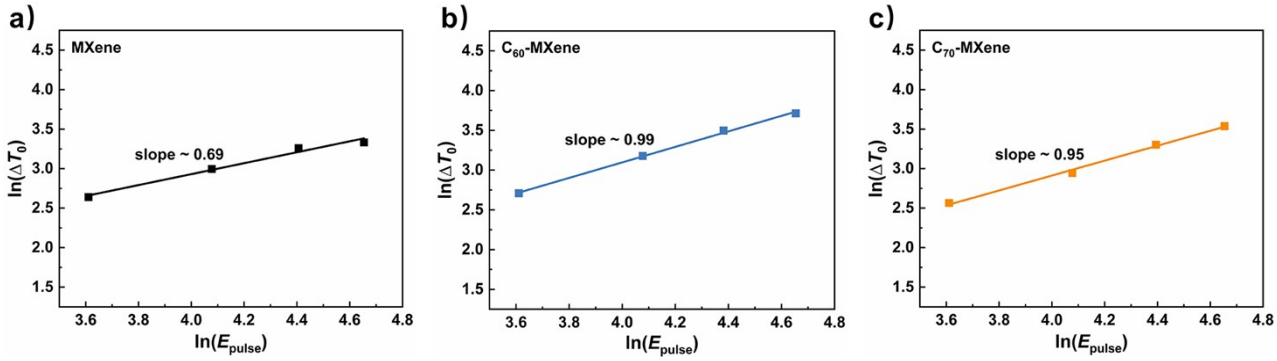

Figure S14. The relationship between ΔT_0 and E_{pulse} in ln-ln scale for a) MXene, b) C_{60}-MXene, and c) C_{70}-MXene based on the Z-scan data under the ns laser irradiation.

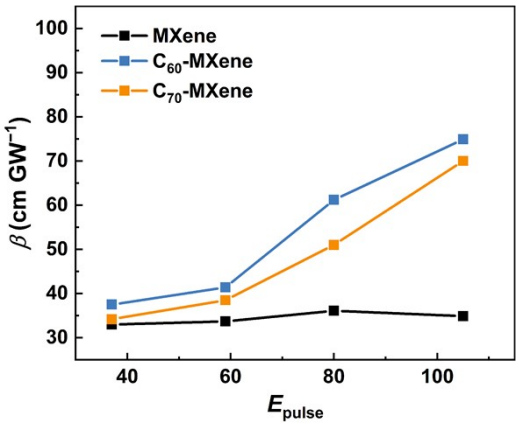

Figure S15. Variation of β of MXene, C_{60}-MXene, and C_{70}-MXene at ns pulses excitation with different E_{pulse}.

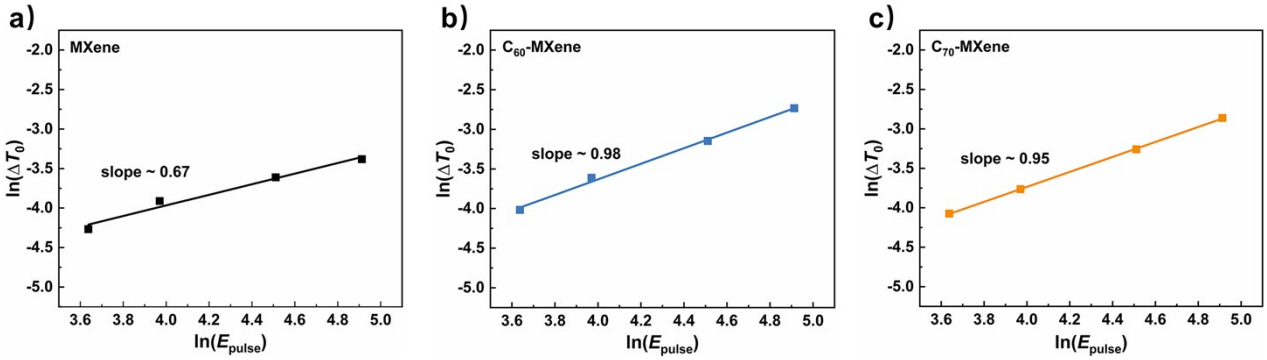

Figure S16. The relationship between ΔT_0 and E_{pulse} in ln-ln scale for a) MXene, b) C_{60}-MXene, and c) C_{70}-MXene based on the Z-scan data under the fs laser irradiation.

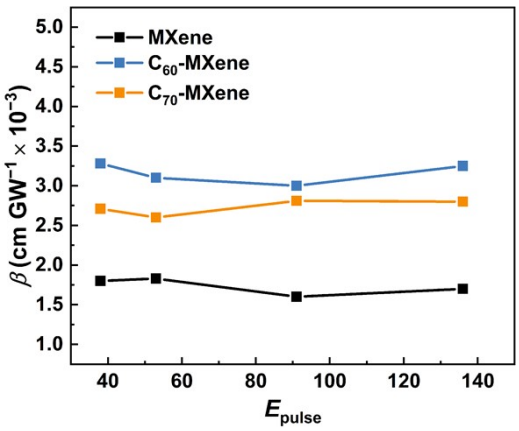

Figure S17. Variation of β of MXene, C_{60}-MXene, and C_{70}-MXene at fs pulses excitation with different E_{pulse}.

References

[1] M. Sheikbahae, A. A. Said, T. H. Wei, D. J. Hagan and E. W. Vanstryland, Sensitive measurement of optical nonlinearities using a single beam, *IEEE J. Quantum Electron.*, 1990, **26**, 760-769.

[2] H. Li, S. Chen, D. W. Boukhvalov, Z. Yu, M. G. Humphrey, Z. Huang and C. Zhang, Switching the Nonlinear Optical Absorption of Titanium Carbide MXene by Modulation of the Surface Terminations, *ACS Nano*, 2022, **16**, 394-404.